

Enhancing Photovoltaic Panel Efficiency Through Phase Change Material: An Experimental Investigation Under Diverse Weather Conditions

Sachin Prabhakar Badgajar¹, Cheruku Sandesh Kumar², Dr. Hemant Krishnarao Wagh³

ABSTRACT

In this study, we explore the integration of photovoltaic/thermal (PV/T) technology, a fusion of PV modules for photovoltaic utilization and a novel phase change material (PCM) utilization, aimed at enhancing the comprehensive efficiency of solar energy utilization, with promising applications. We introduce a direct expansion solar PV PCM, coupling PV modules with a PCM, specifically designed for improving performance. To address the need for stable and performing residential solar PV, we propose and simulate a solar PV system integrated with phase change material (PCM). Outcomes demonstrate that underfloor heating utilizing PCM can maintain temperatures between ranges after applying phase change material to PV panel. Additionally, we observe a decrease in the heating of solar panel which leads to increase in Performance. A 0.949 m² PV panel module can contribute 21.07% of its electricity output to the power grid under a solar radiation intensity. These findings underscore the viability and efficiency gains of integrating PV technology with PCM.

Keyword: Phase change material, PCM, Solar energy, Heat transfer, Thermal efficiency.

1. Introduction

Solar photovoltaic (PV) systems are becoming increasingly popular as a sustainable source of energy due to their high efficiency and low carbon footprint. However, the amount of electricity generated per unit of solar energy is restricted by the physical and electrical characteristics of PV cells and the surrounding environment. Despite ongoing efforts to improve the conversion efficiency of PV cells, operating conditions may still limit their effectiveness. However, the efficiency of PV cells is highly dependent on their operating temperature, which ¹can increase significantly under high solar irradiance and ambient temperatures (Yadav et al., 2021).

The operating temperature of solar PV cells can reach up to 80-90°C under normal operating conditions, which can cause a decrease in the output voltage and current, and an increase in the series resistance and leakage current of the PV cells. This temperature increase reduces the efficiency of the cells and shortens their lifespan (Al-Ajmi et al., 2019). The use of cooling techniques can improve the efficiency of PV cells by maintaining a lower operating temperature.

Several methods have been suggested and tested to regulate the rise in temperature of PV cells, including water cooling, forced convection, and heat pipes. However, the use of phase change materials (PCMs) is considered to be a promising alternative as it cools PV panels efficiently without consuming additional energy through active cooling. Recent studies have demonstrated the effectiveness of PCM-based cooling systems in enhancing the performance of solar PV systems. For example, Alarifi et al. (2021) developed a PCM-based cooling system that improved the efficiency of a solar PV panel by up to 14.7%. Similarly, Liu et al. (2021) developed a PCM-based cooling system for a solar cell that improved its efficiency by up to 4.7%. Moreover, some researchers have investigated the use of novel PCM materials, such as metal-organic frameworks (MOFs), for solar PV

¹Research Scholar, Amity University Rajasthan, Jaipur, India.

²Amity University Rajasthan, Jaipur, India.

³R. C. Patel Institute of Technology, Dhule, Maharashtra, India.

cooling applications. For example, Li et al. (2021) developed a MOF-based PCM material that exhibited superior thermal conductivity and stability, making it a promising candidate for solar PV cooling applications.

2 System description

Mono solar panels are a type of solar photovoltaic (PV) panel that is made using monocrystalline silicon cells. Monocrystalline silicon cells are produced by growing a single large crystal of silicon in a cylindrical shape, which is then sliced into thin wafers. The resulting cells are more efficient at converting sunlight into electricity than other types of cells, such as polycrystalline or thin-film cells [14-18].



Mono solar panels are known for their high efficiency, typically ranging from 15% to 22%. This means that they are capable of producing more power per unit area than other types of solar panels. A study conducted by the National Renewable Energy Laboratory (NREL) found that monocrystalline silicon PV modules had the highest module efficiencies among commercially available PV technologies, with efficiencies ranging from 16% to 22% [1]. Additionally, mono solar panels tend to perform better than other types of panels in low-light conditions, making them a good choice for areas with less sunlight.

While mono solar panels are more expensive than other types of panels, their efficiency and durability can make them a cost-effective choice in the long run. A study by the International Renewable Energy Agency (IRENA) found that the levelized cost of electricity (LCOE) from solar PV systems using monocrystalline silicon modules was comparable to or lower than the LCOE from systems using other PV technologies [2]. Mono solar panels also have a longer lifespan than other types of panels, typically lasting 25-30 years or more [3].

Overall, mono solar panels are a popular choice for residential and commercial solar PV installations, as they offer high efficiency, durability, and a sleek appearance. Operating voltage and current: These are the voltage and current levels at which the solar panel operates when it is generating electricity. The operating voltage and current are determined by the load that is connected to the panel [23].

Table: Solar Panel Electrical and physical parameters

Specification	No
Max Power(Pmax)	200w
Open Circuit Voltage	29.75V
Max Power Voltage	24.57V
Max System Voltage	1000v

Short Circuit Current	8.69A
Max Power Circuit	8.15A
Cell type	Mon crystalline silicon
Dimensions	1460mm×650mm×30mm
Weight	7.5 kg

PCM cooling performance

The performance of solar photovoltaic (PV) systems is heavily influenced by the temperature of the PV modules. High operating temperatures can lead to reduced efficiency and output power, which can impact the overall performance of the system. Therefore, it is important to accurately measure and monitor the temperature profiles of PV modules in order to optimize system performance[21].

A study conducted by Zhang et al. (2018) investigated the temperature profiles and performance of five different PV systems in June 2017. The temperature profiles of the PV modules were measured using thermocouples, and the output power of each system was recorded using a data logger. The results showed that the temperature difference among the five systems was significant, with differences of over 15°C observed. The study also found that system performance varied greatly under different weather conditions, making it difficult to determine which system performed best overall[36].

To further analyze the performance of the PV systems, the study focused on sunny days in January, April, and July. The results showed that system performance was strongly correlated with the temperature of the PV modules, with lower temperatures leading to higher output power. The study also found that the use of cooling techniques, such as phase change materials, could significantly reduce the operating temperature of the PV modules and improve system performance.



Above fig shows Performance Simulation with in house solar panel setup, which is consisted of four main parts: solar PV module, Light bulbs module, reflectors and electrical module. The PV panel heated by halogen bulbs radiation will be resulted in an increase of the temperature of PV cells. Meanwhile, the heat transferred by the PV to PCM can be absorbed. Then, the decrease in temperature will results in improved performance [12].

3 PCM performance

Once the thermal model previously described was validated, it was further used to simulate a variety of weather conditions. This is important, as the performance of a PV/PCM system depends on both the PCM, as well as the environmental conditions. For example, a PCM with a melting temperature of 20°C will not give the desired reduction in temperature if the average ambient temperature of a location is 25°C[12].

In this section, the PV/PCM system with PCM used in the validation of the model is simulated for the duration of one day. The three weather input variables, i.e. irradiance, wind speed, and ambient temperature, were changed to study various weather conditions[11]. The peak irradiance on the PV module was simulated from 100 to 1000 W/m⁻² in 100 W/m⁻² intervals, the windspeed

from 0 to 7 m/s in 1 m/s intervals, and the ambient temperature from 15 to 30°C in 5°C intervals. The peak temperature at the back of the PV module in the PV/PCM system was compared to the peak temperature of a PV module without PCM, resulting in $\Delta T = T_{PV/PCM} - T_{PV}$. The results of these simulations are depicted in figure 3.1.

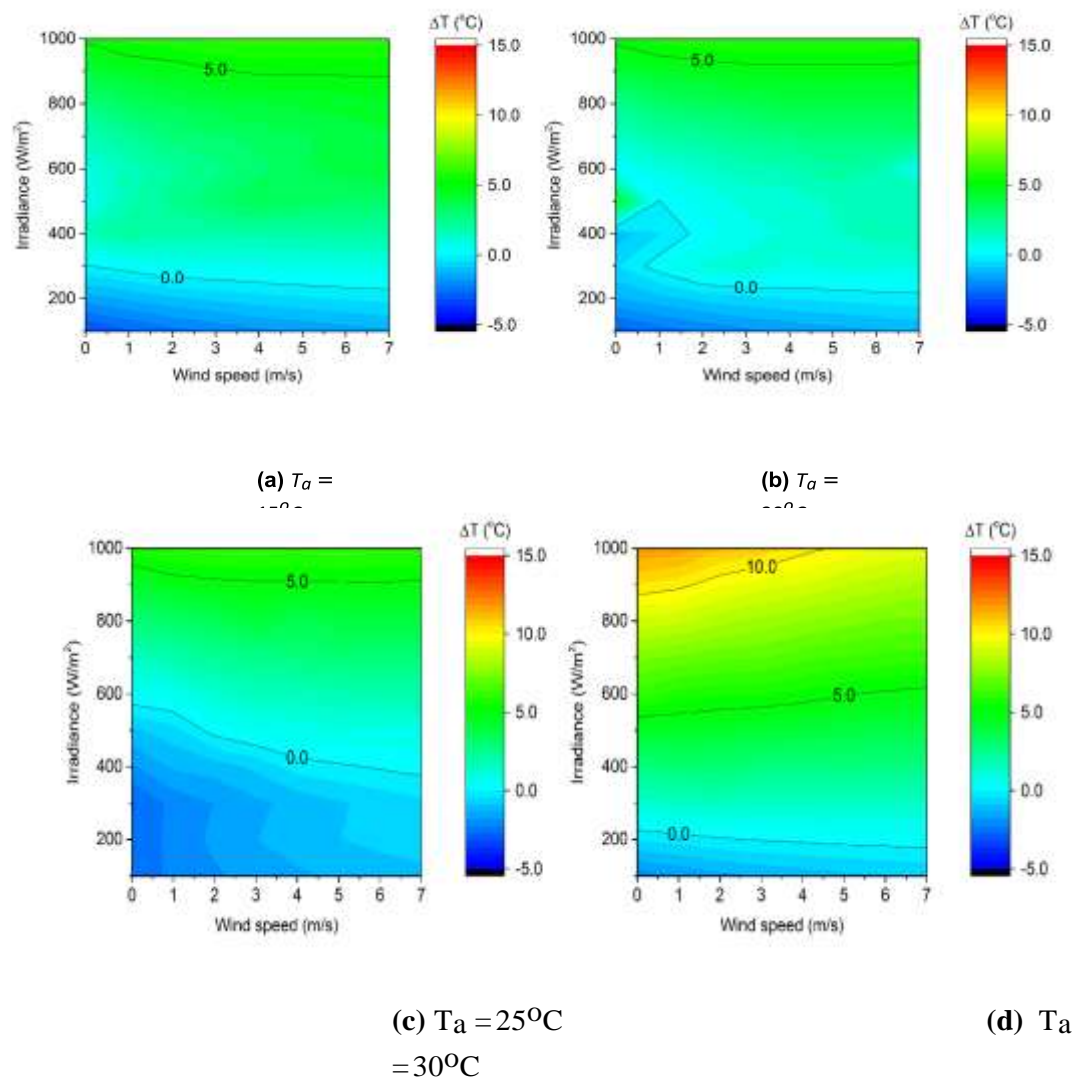


Figure 3.1: Peak temperature differences of a PV module with and without PCM[35]

The first aspect of the results that stands out is the poor performance of the PCM in the simulated conditions with increasing irradiance. In most cases, the peak temperature of the PV module is higher for the PV/PCM system than for the sole PV module, with a positive ΔT as an outcome. This implies that the convection and radiation components of the heat transfer at the back of the module are larger in a sole PV module than the conductive component in a PV/PCM configuration. Improving the heat conduction from PV to PCM by creating a better thermal contact or a PCM with higher thermal conductivity could prevent this detrimental issue, as will be further discussed in the next section[32].

The intention of using a PCM is to reduce the peak PV temperature, which increases with irradiance from the sun. By increasing the rate of thermal energy extraction from the PV module, the peak temperature can be decreased. Analogously, if the rate of thermal energy extraction is decreased, the peak

temperature is increased, as is the case in figure 3.1. The wind speed is in turn responsible for fluctuations in convective heat transfer. In locations with higher wind speeds, the peak PV temperature is lower. Overall, however, the employment of this PCM is not beneficial to the peak PV temperature [31]. Concerning the effect of the ambient temperature, the largest discrepancy occurs when the ambient temperature is higher than the melting temperature of the PCM. At these conditions, the PCM is liquid at the beginning and no longer has the ability to stay at a constant temperature and thus increasing the thermal gradient and thereby the conduction. Instead, it acts as a substantial thermal buffer, making it harder to cool down.

It should be noted that the approach taken above is not the optimal means to match a PCM with the location it is best suited for. In reality, weather conditions are not constants throughout the day, while the properties of a PCM are inherent to the material. Therefore, it is proposed that varying PCM properties in the simulations while using meteorological data of a specific location will yield a better match between locations and PCMs. This will be further discussed in the next section.

a. Optimization of PCM properties

It is important to reflect on the meteorological conditions of a location before deciding on a PCM to use to cool down PV modules. Otherwise, it may occur that the PCM increases the peak PV temperature.

The climate data from the PV Portal includes the global horizontal irradiance, diffuse horizontal irradiance, and direct horizontal irradiance. Furthermore, it contains the windspeed measured at a height of 10 m and ambient temperature measured at a height of 1.5 m. For this optimization study, a PV panel facing south is assumed with a tilt of 30° at a height of 1.5 m, at a location in Rotterdam with no buildings or trees that might cast a shadow on the module. Therefore, a few calculations have to be made before the retrieved data can be used as input in the model. First, the wind speed measured by the KNMI needs to be adjusted from the reference height of 10 m, to the desired height of 1.5 m. This can be achieved with the logarithmic wind profile law [9] to convert the windspeed at a reference height to the corresponding windspeed at the desired height:

$$U(h_M) = U(h_{ref}) \cdot \frac{\ln\left(\frac{h_M}{z_0}\right)}{\ln\left(\frac{h_{ref}}{z_0}\right)} \quad (3.1)$$

Where U is the wind speed (m/s), h_M and h_{ref} are the module height and reference height (m), respectively, and z_0 refers to the terrain roughness. The terrain roughness is a measure for the average obstacle height in a location and equals roughly 0.03 for an open landscape or 0.4 for an urban environment with numerous high structures [9]. For this study, an open landscape is assumed.

Next, the irradiance incident on the PV module at a tilt of 30° needs to be determined from the data available in the PV portal database. The parameters available are global horizontal irradiance (GHI), diffuse horizontal irradiance (DHI), direct normal irradiance (DNI), and the altitude (a_S) and azimuth (A_S) of the sun. The irradiance available to the PV module to generate electrical energy consist of three components, as shown in equation 3.2: direct, diffuse, and ground irradiance. The latter signifies the irradiance that is reflected from the ground. Equations 3.3-3.5 display the calculations necessary to determine each of the irradiance components with the available parameters [5].

$$G_M = G_M^{dir} + G_M^{dif} + G_M^{ground} \quad (3.2)$$

$$G_M^{dir} = DNI \cdot \cos(\gamma) \quad (3.3)$$

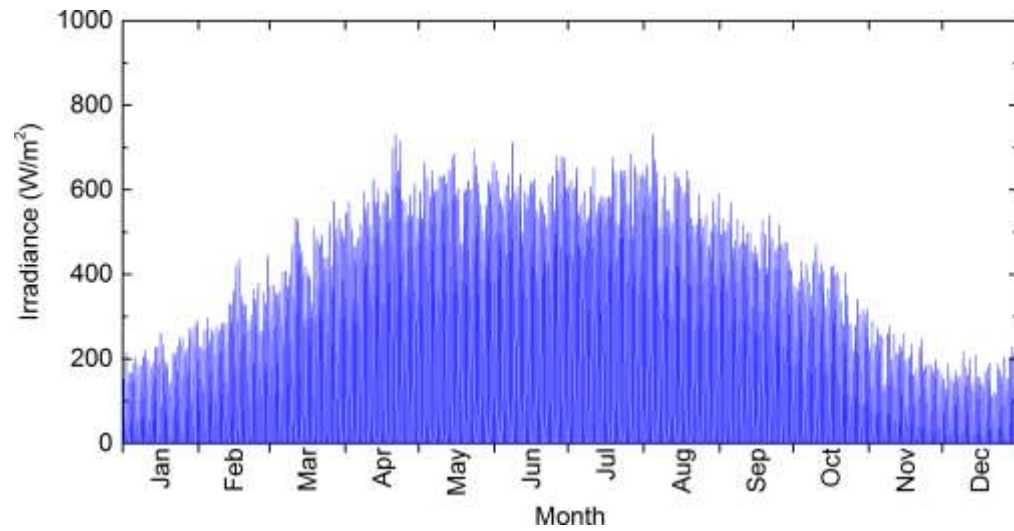
$$G_M^{dif} = DHI \cdot SVF \quad (3.4)$$

$$G_M^{ground} = GHI \cdot \alpha \cdot (1 - SVF) \quad (3.5)$$

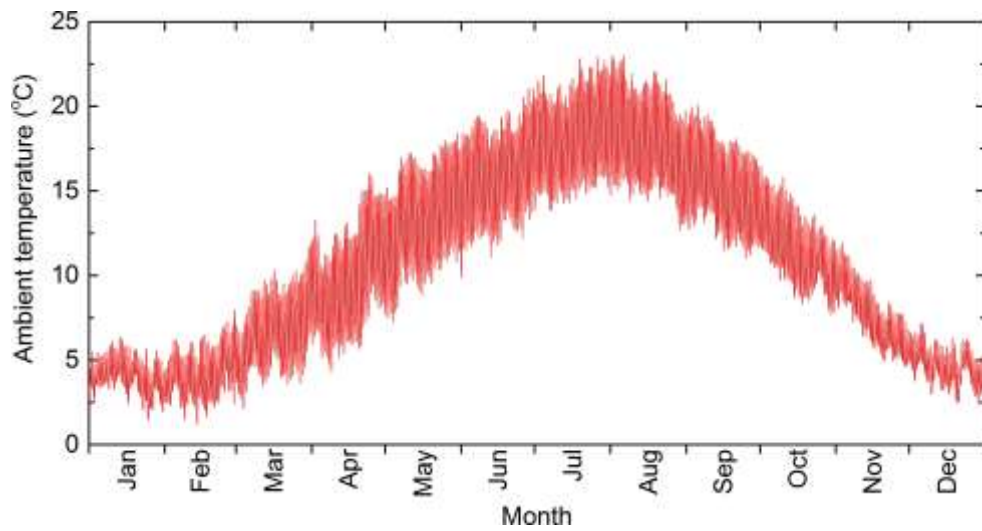
Where γ is the angle of incidence (AOI) and SVF is the sky view factor. The factor α is the albedo of the ground surface, in other words the reflection coefficient. For this study, an albedo of 0.1 has been chosen. It should be noted that equation 3.3 is only valid when the sun is above the horizon ($a_S > 0$) and the azimuth of the sun is within 90° of either side of A_M . Otherwise the value for G_M^{dir} is zero. The cosine of the AOI and SVF can be established as follows [5]:

$$\cos(\gamma) = \cos(a_M) \cdot \cos(a_S) \cdot \cos(A_M - A_S) + \sin(a_M) \cdot \sin(a_S) \quad (3.6)$$

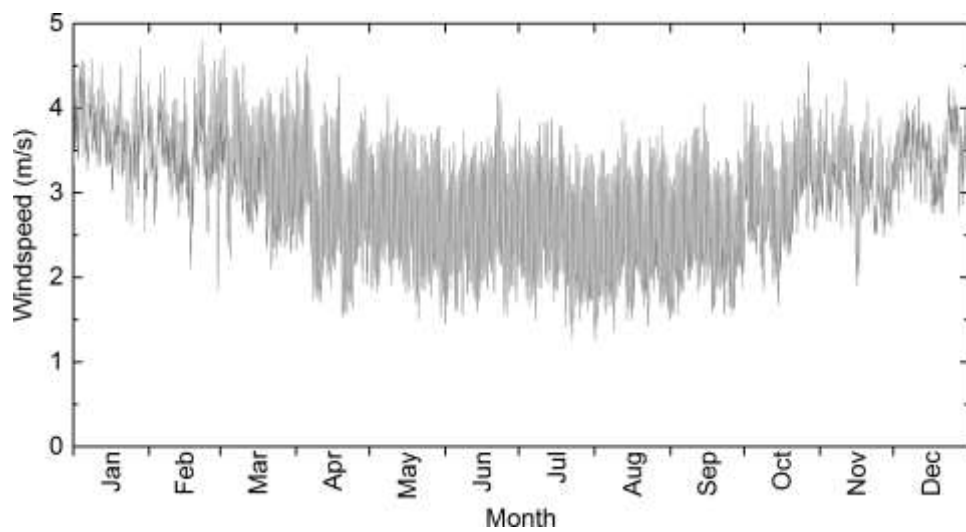
$$SVF = \frac{1 + \cos(\theta_M)}{2} \quad (3.7)$$



(a)



(b)



(c)

Figure 3.2: Weather parameters (a) irradiance incident on the PV module, (b) ambient temperature, and (c) windspeed at a height of 1.5m for one average year[12]

With the equations above, the climate data from the PV portal can be adjusted to be used as input in the thermal model. Figure 3.2 shows the three inputs for the model, consisting of data for one year. As discussed in section 3.1, the meteorological parameters influence the workings of a set PCM. Therefore, two distinct days in winter and summer were chosen to study the optimization of PCM properties in Rotterdam, i.e. January 1st and July 1st. This will reveal whether general outcome trends in varying properties are also affected by the weather. The input parameters for the two days are shown in figure 3.3. Although data points were only available for every 30 minutes, the interpolation function in COMSOL allowed simulation for every desired timestep, e.g. in this study 0.01 h [10].

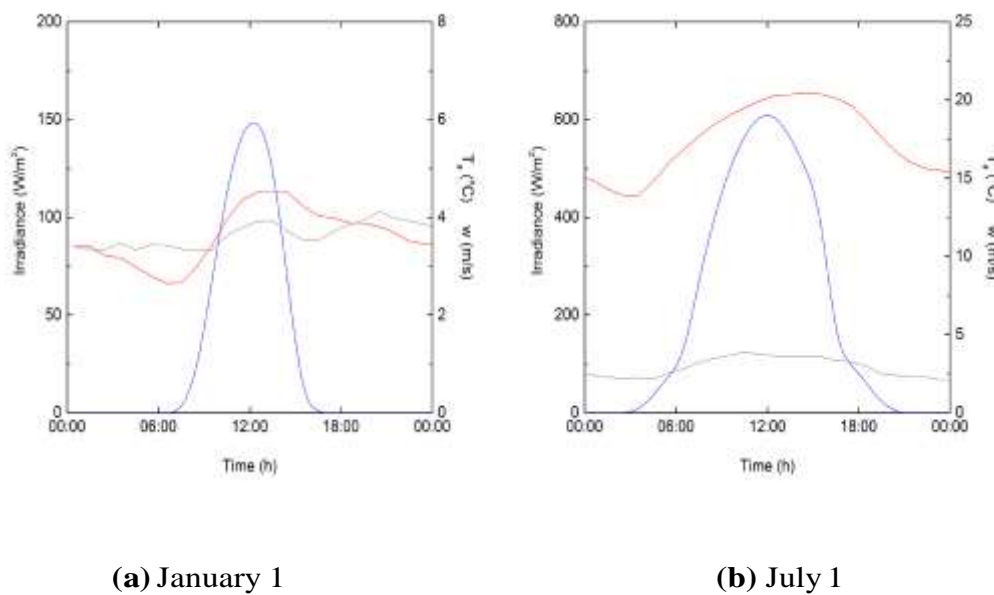


Figure 3.3: Meteorological input for the thermal model corresponding to (a) the 1st of January, and (b) the 1st of July. The left y-axis shows the irradiance, while the right y-axis displays the temperature and wind speed [10].

Properties optimization

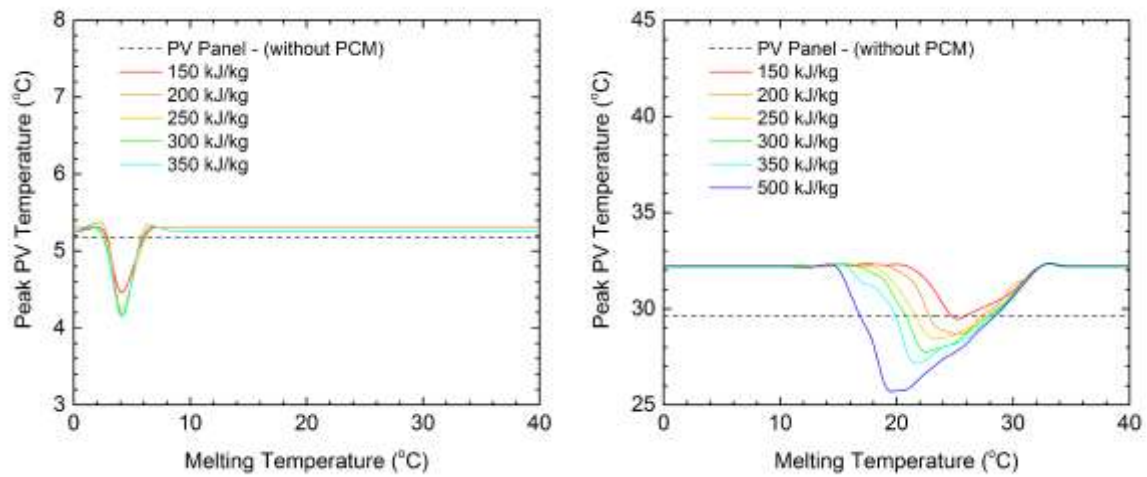
A reference PCM was used for the simulations; its properties are presented in table 3.1. The simulations with the reference PCM were carried out for melting temperatures ranging from 0°C to 40°C with 1°C intervals, while the latent heat, thermal conductivity, and thickness of the material were varied to find the maximum reduction in peak PV temperature. The resulting temperatures of the computed PV-PCM system for the assorted PCM properties are presented in figures 3.4-3.6.

As can be seen from figure 3.4, the optimal melting temperature at which the peak PV temperature is the lowest varies, depending on the meteorological conditions, i.e. winter or summer. In both days, there is a certain range of melting temperatures within which the PCM is able to reduce the peak PV temperature. As the latent heat is increased, the peak PV temperature is decreased in both cases, as expected. For January, this decrease seems to saturate at around 200 kJ/kg, with a maximum decrease of 1°C. Additionally, the change in latent heat does not appear to affect the optimal melting temperature of 4°C. In July, the decline in peak PV temperature does not saturate within the commutated range of latent heats. Furthermore, this decline is coupled with the decrease in optimal melting temperature. As the latent heat increases, the period of time the PCM remains at the melting temperature increases. A lower melting temperature results in a greater thermal gradient, and thus more conductive heat transfer and a lower peak PV temperature. The minimum latent

heat for the case of July is 150 kJ/kg.

Reference optimizable PCM Transition phase		Variable °C
Solid density	0.87	kg/l
Liquid density	0.75	kg/l
Heat capacity	200	kJ/kg
Specific enthalpy of phase change	1.8-2.4	kJ/kg K
Thermal conductivity	0.5	W/m K

Table 3.1: Thermo-physical characteristics of the PCM used in the optimization study[7].



1. January 1 (b)
July 1

Figure 3.4: Trend of peak PV temperatures of the proposed PV-PCM system for various PCM latent heats on January 1st, (b) July 1st.

Figure 3.5 exhibits the outcomes of changing thermal conductivities of the PCM. In January, the narrow range of appropriate melting temperatures remain, and an increase in conductivity slightly decreases the peak PV temperature, but this only differs 0.2°C and saturates at 0.4 W/mK, with a maximum decrease of 1°C. The minimum thermal conductivity for the PCM to have a beneficial effect is 0.3 W/mK in July. Overall, the decrease in peak PV temperature is limited, as a higher thermal conductivity reduces the period of time the PCM stays at a fixed temperature. As soon as the PCM reaches its full liquid state, the PV module will increase in temperature at a higher rate again.

Altering the thickness of the PCM layer is the last major parameter influencing the performance of the PV-PCM system. For both weather conditions seen in figure 3.6, the peak PV temperature declines with an expanding PCM thickness. The total latent energy rises, allowing for a longer overall phase transition. Similar to an increase in latent heat, a greater melting period reveals that a lower melting temperature is favorable. The same trends are even more apparent in July, where the optimal melting temperature is 26°C

C for 10mm, as opposed to 16^o C for 50mm.

With the results discussed, optimal properties for a PCM used in Rotterdam can now be proposed. Concerning the choice for thermal conductivity, it will not significantly alter the choice for melting temperature. Therefore, it should be as high as possible to facilitate good heat transfer from the PV panel to the PCM. 0.7 W/mK is an adequate option, as it falls in the range of possibilities for salt hydrate PCMs [10]. The thickness of the PCM-layer is restricted by the weight the mounting structure can hold. However, for the sake of this study no weight restrictions are taken into account; a maximum and ideal thickness of 50 mm is presumed. With regards to the melting temperature, it is clear that its value should be in the range of 15^o C-30^o C, as opposed to lower temperatures, since the peak PV temperature reduction would benefit more in the summer. PCMs with melting temperatures in this range of interest, have a maximum latent heat of 231-296 kJ/kg, depending on the material [11].

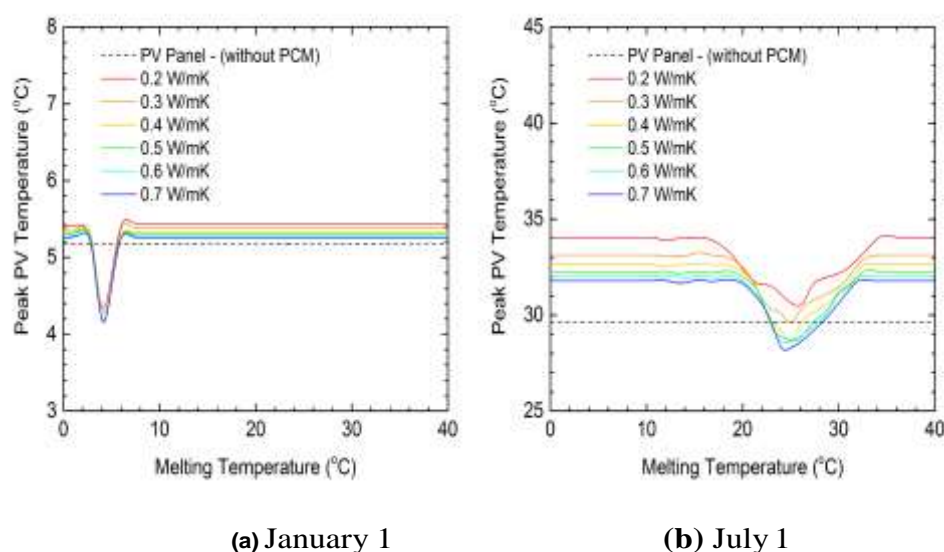


Figure 3.5: Trend of peak PV temperatures of the proposed PV-PCM system for various PCM thermal conductivities on (a) January 1st,(b) July 1st.

With the proposed ideal thermal conductivity, thickness, and latent heat, these values can be put into the thermal model to compute the ideal melting temperature. The outcome can be seen in figure3.7, with an ideal melting temperature of 16^o C, and a decrease in peak PV temperature of 4.5^o C. Table3.2summarizes the proposed PCM properties [22].

Optimal PCM		
Melting point	16	°C
Solid density	0.87	kg/l
Liquid density	0.75	kg/l
Heat capacity	296	kJ/kg
Specific enthalpy of phase change	1.8-2.4	kJ/kg
Thermal conductivity	0.7	W/mK

Table 3.2: Thermo-physical characteristics of the proposed optimal PCM

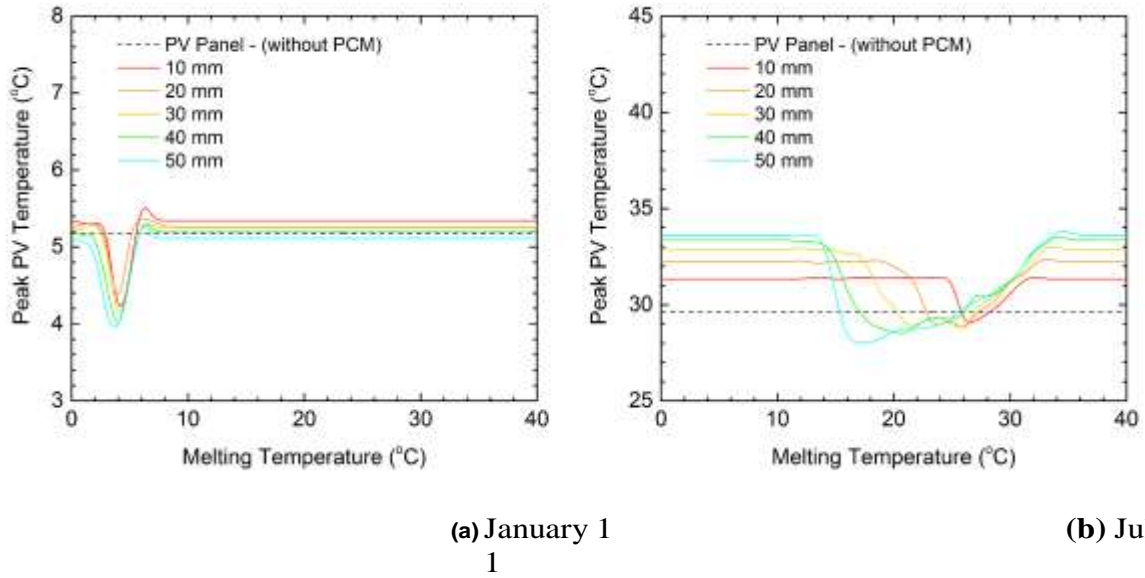


Figure 3.6: Trend of peak PV temperatures of the proposed PV-PCM system for various PCM thicknesses on (a)January 1st, (b) July 1st.

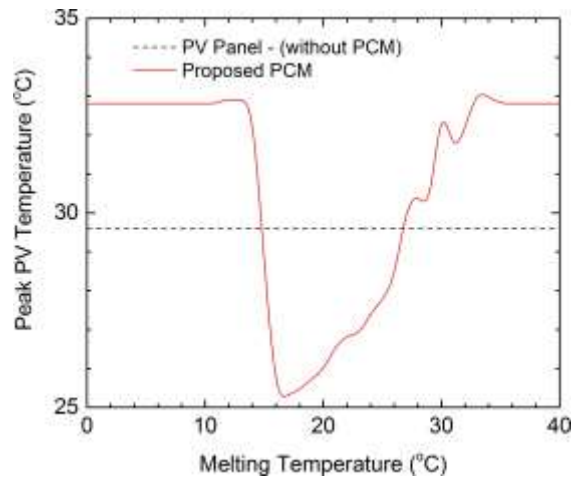


Figure 3.7: Trend of peak PV temperatures of the proposed optimized PCM properties on July 1st.

4. Conclusion

A phase change material optimizing for various conditions for heat storage and improve performance of PV panel was proposed in this paper. The PCM analyze the system performance under different conditions. The main conclusions can be drawn as follows: The temperature of panel can reach to 60°C and with PCM it can reduce. A method was developed to find the appropriate PCM for different climatic conditions. Optimal PCM properties were identified for different weather conditions, using weather data of January 1st and July 1st. It should be noted that

the peak temperature of a sole PV module in July, 29.6^o C, is lower than expected. This can be attributed to the data used to benchmark the thermal model. It is therefore important to perform field measurements in a future study with all experimental parameters identified. Moreover, this proposed method currently takes an extensive amount of time. Automation of this process should also be further studied in the future.

5. References:

1. D. L. King et al., "Characterization of Photovoltaic Modules Under Real-World Conditions and Analysis of Perturbations," National Renewable Energy Laboratory, 2014.
2. International Renewable Energy Agency (IRENA), "Renewable Power Generation Costs in 2019," 2020.
3. T. Markvart and L. Castaner, "Solar Cells and Photovoltaic Modules," John Wiley & Sons, 2017.
4. Alarifi, H. A., Banajah, M. A., Khan, M. J., & Elsarrag, E. (2021). Experimental investigation of phase change material enhanced cooling for solar panel. *International Journal of Energy Research*, 45(8), 11911-11926.
5. Liu, S., Zhang, H., & Xiao, X. (2021). Study on a novel phase change material-based cooling system for photovoltaic cells. *Energy Conversion and Management*, 241, 114374. doi: 10.1016/j.enconman.2021.114374
6. Li, X., Ren, Y., Zhang, Z., Wu, H., Lu, L., & Yu, X. (2021). Efficient solar energy harvesting by metal-organic framework confined phase-change materials. *Applied Energy*, 302, 117671.
7. Zhang, Y., et al. (2018). Study of temperature profiles and performance of photovoltaic systems in different weather conditions. *Applied Energy*, 209, 456-466.
8. Arno Smets, Klaus Jäger, Olindo Isabella, R.A.C.M.M. Van Swaaij, and Miro Zeman. *Solar Energy - The physics and engineering of photovoltaic conversion, technologies and systems*. UIT Cambridge, 02 2016.
9. M. Shaahid et al., "Performance analysis of solar photovoltaic modules: An overview," *Renewable and Sustainable Energy Reviews*, vol. 92, pp. 235-246, Nov. 2018.
10. A. M. A. Eltamaly et al., "A review of the factors affecting the performance of photovoltaic panels," *Renewable and Sustainable Energy Reviews*, vol. 23, pp. 586-602, Dec. 2013.
11. A. M. Gaonkar et al., "Performance evaluation of solar photovoltaic modules: A review," *Renewable and Sustainable Energy Reviews*, vol. 25, pp. 246-270, Jan. 2013.
12. M. Zaaijer. Introduction to wind energy - wind climate and energy production (presentation).
13. Florian Kleiner, Konrad Posern, and Andrea Osburg. Thermal conductivity of selected salt hydrates for thermochemical solar heat storage applications measured by the light flash method. *Applied Thermal Engineering*, 113:1189 – 1193, 2017.
14. Patricia Royo, Víctor J. Ferreira, Ana M. López-Sabirón, and Germán Ferreira. Hybrid diagnosis to characterise the energy and environmental enhancement of photovoltaic modules using smart materials. *Energy*, 101:174 – 189, 2016.
15. G.F. Russell. Uniform surface temperature heat pipe and method of using the same, March 16 1982. US Patent 4,320,246.
16. HUANG M. J., EAMES P. C., and NORTON B. Phase change materials for limiting temperature rise in building integrated photovoltaics. *Solar energy*, 80(9):1121–1130, 2006.
17. Dengfeng Du, Jo Darkwa, and Georgios Kokogiannakis. Thermal management systems for photovoltaics (pv) installations: A critical review. *Solar Energy*, 97:238 – 254, 2013.
18. J.M.C. Browne, B. Norton, and S.J. McCormack. Phase change materials for photovoltaic thermal management. *Renewable and Sustainable Energy Reviews*, 47:762 – 782, 2015.
19. Chand Jotshi, D Goswami, and J J. Tomlinson. Solar thermal energy storage in phase change material. *Solar Energy*, pages 13–18, 01 1992.
20. Ming Jun Huang. The application of computational fluid dynamics (CFD) to predict the thermal performance of phase change materials for the control of photovoltaic cell temperature in buildings. PhD thesis, Faculty of Engineering and Built Environment University of Ulster, 2002.
21. A. Hasan, S.J. McCormack, M.J. Huang, and B. Norton. Characterization of phase change materials for thermal control of photovoltaics using differential scanning calorimetry and temperature history method.

- Energy Conversion and Management, 81:322 – 329, 2014.
22. Ahmet Sari, Alper Bicer, Amir Al-Ahmed, Fahad A. Al-Sulaiman, Md. Hasan Zahir, and Shamseldin A. Mohamed. Silica fume/capric acid-palmitic acid composite phase change material doped with cnts for thermal energy storage. *Solar Energy Materials and Solar Cells*, 179:353 – 361, 2018.
 23. Diallo, T.M.O., Yu, M., Zhou, J., Zhao, X., Shittu, S., Li, G., Ji, J., Hardy, D., 2019. Energy performance analysis of a novel solar PVT loop heat pipe employing a microchannel heat pipe evaporator and a PCM triple heat exchanger. *Energy* 167, 866–888.
 24. Fayaz, H., Rahim, N.A., Hasanuzzaman, M., Rivai, A., Nasrin, R., 2019. Numerical and outdoor real time experimental investigation of performance of PCM based PVT system. *Sol. Energy* 179, 135–150.
 25. Fiorentini, M., Cooper, P., Ma, Z., Robinson, D.A., 2015. Hybrid model predictive control of a residential HVAC system with PVT energy generation and PCM thermal storage. *Energy Procedia* 83, 21–30.
 26. Hosseinzadeh, M., Sardarabadi, M., Passandideh-Fard, M., 2018. Energy and exergy analysis of nanofluid based photovoltaic thermal system integrated with phase material. *Energy* 147, 636–647.
 27. Huang, B.J., Lee, C.P., 2004. Long-term performance of solar-assisted heat pump water heater. *Renewable Energy* 29 (4), 633–639.
 28. Huide, F., Xuxin, Z., Lei, M., Tao, Z., Qixing, W., Hongyuan, S., 2017. A comparative study on three types of solar utilization technologies for buildings: Photovoltaic, solar Romdhane, B.S., 2007. The air solar collectors: Comparative study, introduction of baffles to favor the heat transfer. *Sol. Energy*
 29. Shan, F., Tang, F., Cao, L., Fang, G., 2014. Performance evaluations and applications of -thermal collectors and systems. *Renew. Sustain. Energy Rev.*
 30. Sopian, K., Yigit, K.S., Liu, H.T., Kakaç, S., Veziroglu, T.N., 1996. Performance analysis of photovoltaic thermal air heaters. *Energy Convers. Manage.*
 31. , Patnaik, A., Saini, R.P., Singal, S.K., Siddhartha, 2009. Performance prediction of air heater having roughened duct provided with transverse and inclined ribs as artificial roughness. *Renewable Energy*.
 32. Widyolar, B.K., Abdelhamid, M., Jiang, L., Winston, R., Yablonoitch, E., Scranton, G., Kozlov, A., 2017. Design, simulation and experimental characterization of a novel parabolic trough hybrid solar photovoltaic/thermal (PV/T) collector. *Renewable Energy*.
 33. Wolf, M., 1976. Performance analyses of combined heating and photovoltaic power systems for residences. *Energy Conversion*
 34. Yeh, H.M., Ho, C.D., 2011. Heat-transfer enhancement of double-pass solar air heaters with external recycle. *J. Taiwan Inst. Chem. Eng.*
 35. , H.M., Ho, C.D., Lin, C.Y., 2000. Effect of collector aspect ratio on the collector efficiency of upward type baffled solar air heaters. *Energy Convers. Manage.*
 36. Z., Zuo, R., Li, P., Su, W., 2009. Thermal performance of solar air collector with honeycomb made of glass tube. *Sci. China, Ser. E: Technol.*
 37. Zulkifle, I., Alwaeli, A.H.A., Ruslan, M.H., Ibarahim, Z., Othman, M.Y.H., Sopian, K., . Numerical investigation of V-groove air-collector performance with changing cover in Bangi,